ELSEVIER Journal of Hazardous Materials 40 (1995) 213–235

JOURNAL OF HAZARDOUS MATERIALS

The release into the atmosphere of hazardous volatiles Part I. Release from porous solids imbued with a liquid mixture in which the volatiles are dissolved

Francesco Gioia*, Fabio Murena, Giuseppe Savino, Pratik Saha[1]

Dipartimento di Ingegneria Chimica, Università di Napoli Federico II, Piazzale Tecchio, 80125 Napoli, Italy

Received 27 March 1994; accepted in revised form 1 August 1994

Abstract

An experimental and theoretical study to investigate the release of toxic volatiles from porous media is presented. Three porous media, one synthetic and the other two natural, have been selected. They were imbued in a solution containing toxic volatiles in dilute concentrations. The heavy oily medium used to hold the volatiles in the liquid phase is tetradecane. The toxic volatiles whose diffusion is studied include benzene, chlorobenzene and 1,3-dichlorobenzene. These chemicals were chosen so that a wide range of volatilities could be studied.

Two different desorbers have been used. The first is a desorption chamber containing a single sphere of the porous medium. The second, more suitable for studying the diffusion of the less volatile components, has a cylindrical fixed bed geometry in which smaller porous spheres are arranged.

The theoretical tools used to model the diffusion process show good accuracy in describing the experimental data.

1. Introduction

The prerequisite for modeling the dispersion into the atmosphere of volatile pollutants from contaminated soils is to define clearly the mechanisms which rule the diffusion of the volatiles inside the porous particles which form the soil.

Many authors (e.g., [1–9]) have investigated the overall air emission of hazardous organics from soils. A summary of the various predictive models for estimating air emissions, dated 1985, is presented by Balfour et al. [10]. A review paper on the

* Corresponding author. Fax: (+ 39-81) 239-1800. Tel.:(+ 39-81) 768-2277.

[1] Student participating in the ERASMUS programme (ICP n. 92-I-1006/06) of the Commission of the European Communities. From University College, London.

0304-3894/95/$09.50
SSDI 0304-3894(94)00083-2

currently postulated transport mechanisms is presented by Thibodeaux et al. [5]. Little attention has been, however, devoted to the investigation of the mechanisms which rule the diffusion inside the single particles which form the soil. In many cases, in order to avoid awkward predictive equations for the overall release model, the investigators account for this diffusion in the most simple way. For example, Thibodeaux and Hwang [1] in formulating the air emission release rate (AERR) model reduce the diffusion of the volatiles inside to the porous particles to a diffusion through an hypothetical film which coats the soil particles. Actually, the knowledge of the diffusion mechanisms inside the single particles is important because it represents the first step of the overall air release process.

The problem of diffusion in porous solids is of fundamental interest in many areas of chemical engineering and much research has been devoted to the subject. However, only one paper [11] has been published recently which investigates on the transient liquid phase diffusion in a porous medium. In particular the authors focus attention on the two-phase diffusion in the voids of a bed of nonporous glass spheres.

Indeed, investigations on the liquid phase diffusion in porous solids would be of prevailing interest in the area of environmental engineering. In the present paper we investigate, both theoretically and experimentally, the fundamental aspects of the transient diffusion inside particles of porous materials imbued with a liquid waste. The model waste is an oily medium of low volatility (tetradecane) in which toxic volatile substances are dissolved. The low volatility of the medium allows us to consider it to be immobile during the mass transfer process.

The experiments are conducted with closely controlled geometry, porous structure and nature of the porous material, and fluodynamics, so as to keep to a minimum the uncertainties in the predictive equations and focus attention on the role played by the transport phenomena taking place inside the porous material. Three porous media are studied. The first is a synthetic one, i.e., sinterized porous stainless steel (SS). The other two are natural porous rock, i.e., yellow and grey tuffs. The purpose of studying the diffusion inside a porous SS is to define experimentally the role played by microporosity and surface migration on the overall diffusion process. Our experiments allow us to exclude a significant role of both. In the SS, microporosity is absent and surface adsorption may be considered negligible (thus surface migration must be negligible too). In the tuffs, microporosity is present and adsorption might play a role too. Comparison between the result for the SS and those obtained for the natural rock indicate that the effect of microporosity and surface migration on the overall diffusion is not detectable.

Two different desorbers are utilized. In the first, a single large sphere of the selected porous material is contained. In the second, smaller tuff spheres are arranged in a cylindrical fixed bed geometry.

The liquid mixture simulating the waste imbuing the spheres is a mixture of organic volatiles in tetradecane. The toxic volatiles, whose diffusion is studied, include benzene, chlorobenzene and 1,3-dichlorobenzene. These chemicals were chosen so that a wide range of volatilities could be studied.

The following sets of experiments have been accomplished: (1) Release of benzene from a single sphere of porous material (both natural and synthetic) imbued with

mixtures of benzene in tetradecane [12]. (2) Release of benzene, chlorobenzene and dichlorobenzene in an admixture with tetradecane from spheres of porous natural material in a packed bed arrangement [13].

2. Experimental procedure

The porous medium chosen is imbued in a liquid solution that contains the toxic compound/s. Then it is introduced into a desorption chamber in which nitrogen is flowing at a given flow rate. The diffusion of the volatiles to the gas phase is studied by measuring the concentration of the volatiles with time in the gas leaving the desorber. Details are as follows.

2.1. Single sphere experiments

A sphere (diameter 27 mm) of porous material is used to run these experiments. Three different porous materials are used: sinterized SS and two types of natural rock (yellow tuff and grey tuff). The purpose of using the SS is to check for the effects of adsorption, surface migration and microporosity on the transport mechanism. In fact, for the the SS sphere these effects may be assumed to be absent while for the tuffs they might play a role. The SS powder used to mold the sphere before the sinterization consists of spherical particles having a diameter of 300 μm. The internal structure of the yellow tuff is characterized by a mercury porosimeter: the total porosity ε_t is 0.38, 16% of which is taken up by the microporosity ε_i, in the range ($50 < r_c < 600$ Å) having a maximum frequency at $r_c = 200$ Å. The macroporosity ε is in the range $1000 < r_c < 50{,}000$ Å with a maximum frequency at 10,000 Å.

Because the single grains forming the sinterized SS sphere are nonporous, the sphere shows a unimodal pore size distribution with a porosity ε essentially due to interparticle voids.

The relevant structural characteristics of the three materials are reported in Table 1. The porosity of the SS sphere has been calculated according to the relationship:

$$\varepsilon = 1 - \frac{\rho_b}{\rho_p}, \tag{1}$$

where ρ_p is the true density of SS equal to 7.7 g/ml and ρ_b is the bulk density determined as 2.81 g/ml.

The oily mixtures which simulate the waste are solutions of benzene (the diffusing chemical) in tetradecane. Tetradecane is involatile and therefore does not transfer into the gas phase during the experiments (at 19 °C the vapour pressure is 6.4×10^{-6} atm). Runs have been performed with several initial benzene concentrations, in the range $0.1 \leqslant x_b \leqslant 1$. The runs that will be considered in this paper are those in the range $0.1 \leqslant x_b \leqslant 0.2$. Runs with larger benzene concentrations up to $x_b = 1$ are reported and discussed in the thesis of Savino [12] .

Table 1
Materials and operating conditions for the various runs

Run no.	Porous material	$\varepsilon + \varepsilon_i$	ρ_a (g/ml)	T (°C)	Q (ml/s)	x_b (mol frac.)	x_{cl} (mol frac.)	x_{dcl} (mol frac.)
Sp-1	SS	0.63	2.81	17	1.0	0.1	—	—
Sp-2	SS	0.63	2.81	22	10.0	0.2	—	—
Sp-3	GT	0.55	1.56	26	10.0	0.2	—	—
Sp-4	YT	0.38	1.09	26	10.0	0.2	—	—
Pb-1	YT	0.38	1.09	19	13.3	0.2	—	—
Pb-2	YT	0.38	1.09	19	13.4	0.1	0.1	—
Pb-3[a]	YT	0.38	1.09	19	13.6	—	0.1	—
Pb-4	YT	0.38	1.09	19	13.9	—	0.1	—
Pb-5	YT	0.38	1.09	19	13.7	—	0.1	0.1
Pb-6	YT	0.38	1.09	19	13.9	0.1	0.1	0.1
Pb-7[b]	YT	0.38	1.09	24	13.4	0.1	0.1	0.1

Sp: single sphere; Pb : packed bed; SS : porous stainless steel; GT : grey tuff; YT : yellow tuff.
[a] Wet spheres scattered before insertion in the desorber; therefore $\phi = 1$.
[b] Height of the bed 2 cm instead of 6.2 cm as for all the other Pb runs.

The desorption chamber is made of glass and has a volume of 113 ml. Nitrogen gas enters the desorption chamber through the bottom of the apparatus where it passes through a glass porous set. The porous set, with a thickness of 4 mm, serves the purpose of making uniform the flow of gas. The flowrate of gas through the system is measured by a bubble flow meter that is connected to the top of the desorption chamber. Also present in the system above the sphere, to check temperature changes, is a thermocouple. See Fig. 1(a) for a schematic view of apparatus.

The solution of tetradecane having the desired benzene concentration is put in a glass cylinder. The sphere is then hooked onto the end of a long thin piece steel wire that is held firm through a small bore drilled along the axis of a silicon cork. The sphere is then lowered into the mixture until fully submerged. The cork covers the top of the cylinder thus rendering it gas-tight and leaving the vacant head above the liquid level saturated by vapours from the solution. The sphere is left immersed for 24 h after which the wire is pulled up through the silicon cork. Thus the sphere is left in the space above the liquid level in order to drain off any excess fluid. As soon as the cork is removed the sphere is rapidly weighed and hang into the desorption chamber where the nitrogen flow is already on. This is the run start time, $t = 0$. The difference between the weight of the sphere after and before the soaking gives the weight of solution which has penetrated it. By the above method we realize a degree of filling which ranges between 80 and 100% of the total porosity.

From the moment of insertion of the sphere into the desorption chamber samples of exit gas are taken at various times throughout the day. The instantaneous samples of gas taken from the exit stream are extracted from a specific length of rubber tube using a gas-tight syringe with a capacity of 1 ml, supplied by Dynatech. This piece of tube forms part of the tube length that connects the desorption chamber exit to the flow meter.

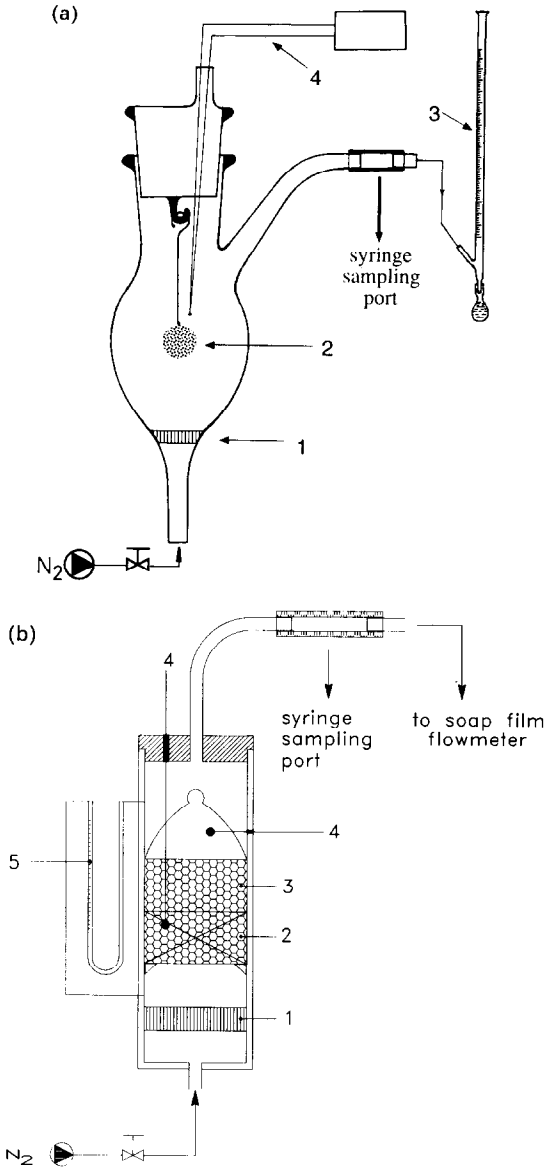

Fig. 1. (a) Desorption apparatus for single sphere experiments. 1 – porous set; 2 – porous sphere; 3 – soap film flowmeter; 4 – thermocouple. (b) Desorption apparatus for packed bed experiments. 1 – porous set; 2 – bed of spheres; 3 – wire grid basket; 4 – thermocouple; 5 – manometer.

The gas phase concentration of benzene in the samples is measured by gas chromatography (Perkin–Elmer 8500). The chromatograph is equipped with a flame ionization detector. The first sample is taken at a time slightly larger than the average residence time of the desorber. To get a better initial resolution of the system, samples

of gas are taken more frequently at the start, i.e., every 3–5 min because the benzene concentration drops rapidly within the first 30 min. Thereafter, the sampling is carried out less frequently. The run is stopped when the benzene concentration in the outlet stream is not measurable. This is the run final time t_f. The parameters that differentiate the runs are the nitrogen flow rate, the initial concentration of benzene in tetradecane and the porous medium. Operating conditions selected for the experimental runs that will be considered in this paper are reported in Table 1. Further details on the experimental apparatus and procedure can be found in the thesis [12].

2.2. Packed bed experiments

In these experiments attention is focused on mixtures having low concentrations of volatiles ($x_i \leqslant 0.1$). The single sphere experiments are not suitable to study the release mechanism of compounds having volatility much lower than that of benzene, i.e., chlorobenzene and dichlorobenzene. In fact, due to the low volatility of these compounds, concentrations in the outlet nitrogen stream would be too low to be reliably measured with time. Therefore, a different experimental set up was devised. Namely, a number of spheres of tuff (diameter 4.4 mm) were imbued in the mixture containing the volatiles and arranged in a packed bed with nitrogen flowing through it. By measuring the volatile concentration in the nitrogen outlet stream with time it is possible to infer on the release mechanism from the spheres.

The volatiles whose diffusion mechanisms is studied include: benzene (J.T. Baker Chemicals); chlorobenzene (Aldrich Chemical Co.); 1,3-dichlorobenzene (Aldrich Chemical Co.). Two sets of experiments have been run. The first regards two component mixtures. Namely tetradecane containing either benzene or chlorobenzene. The second set uses mixtures in which two or three contaminating volatiles are present simultaneously in tetradecane. In all cases the mole fraction of each volatile component is 0.1.

For all packed bed experiments yellow tuff is the only porous medium utilized. In fact the single sphere experiments had indicated that the diffusive characteristics of both tuffs are about identical. Furthermore, the experiments using the sinterized SS were carried out with the sole purpose of investigating on the influence of adsorption, surface migration and microporosity on the diffusion mechanism. The single sphere experiments had already shown that this influence is negligible.

The experiments are performed at room temperature in a desorption chamber, a cylindrical column 3.9 cm diameter which is made of Plexiglas, see Fig. 1(b) for a schematic view of apparatus. A cylindrical basket, made of SS wire grid of 2 mm dimension, is constructed in such a way as to sit easily inside the column when filled with spheres. The diameter of the basket is also fixed at 3.9 cm and the height of the basket is 10 cm. The uniform flow of gas then passes through the bed of spheres where the desorption process takes place.

Just above and below the bed of spheres are two openings that lead to a manometer filled with colored water. It is present to monitor pressure drop across the bed. A negligible pressure drop was registered across the bed, and therefore it is assumed that all the experiments took place at atmospheric pressure. Also present in the system

to check temperature changes, are two thermocouples; one has its temperature sensor inside the main body of spheres and the other is just above the bed of spheres. Both thermocouples gave room temperature readings. Thus temperature changes are negligible in all experiments.

The first step at the initiation of each experiment is to prepare the bed by putting the dry spheres into the basket and compacting them well so that they form a uniform cylindrical shape. The basket is weighed and the voidage of the bed can thus be evaluated by an equation analogous to Eq. (1), i.e., $\varepsilon_a = 1 - \rho_a/\rho_b$. ρ_a is the apparent density of the bed and is calculated knowing the mass of the bed of spheres and the volume it occupies in the basket. ρ_b is the bulk density of yellow tuff equal to 1.09 g/ml. The calculated value of the bed voidage ε_a is 0.38.

The solution of the volatiles in tetradecane is prepared according to pre-set mole fraction specifications of the constituents and poured into a 500 ml measuring cylinder. The basket full of spheres is then hooked onto the end of a long thin piece of steel wire that is held firm through a silicon cork. Then the imbuing of the spheres contained in the basket and the start of the run are accomplished using a procedure very similar to that used for the single sphere experiments. Samples of gas in exit are taken at various times throughout the day. Four of the runs, those involving the less volatiles chlorobenzene and 1,3-dichlorobenzene, have been left running overnight, i.e. for 24 h, to see to what extent the concentration levels drop. Operating conditions selected for experimental runs are reported in Table 1. Further details on the experimental apparatus and procedure can be found in the thesis of Saha [13].

3. Theory

The experimental results regarding the single sphere [12] have shown that three different mechanisms can rule the release of a volatile compound from a porous material. They prevail according to the initial concentration of the volatile loaded in the sphere.

– Low volatile concentration ($x_i \leqslant 0.2$). In this case the transport mechanism is a Fickian diffusion through the oily medium which can be considered immobile.

– High volatile concentrations ($0.2 < x_i < 0.8$). Due to the large volume fraction of the volatile in the liquid mixture, during the release process, part of the porosity becomes free of liquid. The experiments have shown that Fick's law may still be used to describe the diffusion inside the porous material. However, the diffusivity must be a weighed average of the liquid and gas phase diffusivities of the volatile. The Millington and Quirk [14] method can be used to calculate this average diffusivity.

– Pure volatile. In this case the movement of volatile is likely to be controlled by surface tension and gravity forces within the solid. Heat transfer phenomena also play a role. The solid temperature changes until it reaches a steady state. The experiments have shown that the drying mechanisms described by Foust et al. [15] apply to the movement of volatile in the sphere.

We will focus attention on the case of low volatile concentrations which better fits the scope of the present paper. The other cases are discussed in a thesis by Savino [12].

3.1. Low volatile concentrations ($x_i < 0.2$)

Single sphere

Because the volatility of tetradecane is much lower than that of benzene, it may be considered immobile. Furthermore, let us introduce the characteristic time for diffusion as:

$$t_d = \frac{l^2}{D_e}, \tag{2}$$

where l is the characteristic dimension of the medium in which diffusion is taking place and D_e is the diffusivity of the chemical. If the observation time t is such that $t \ll t_d$ then the diffusion process may be considered to be in a pseudo-steady-state situation. In our experiments in all cases $t_d \approx t$. Therefore the process is modeled as a transient diffusion of benzene in the tetradecane which fills the porosity of the sphere.

In order to account for the case in which the porous solid has a bimodal pore size distribution (like our tuff rock), we will model the porous material as formed of an ensemble of small microporous grains responsible of the microporosity ε_i while the macroporosity ε is due to the interparticle voids. Naturally for the SS sphere $\varepsilon_i = 0$.

We use spherical coordinates. The diffusion of benzene along the r direction can be assumed to take place essentially through the macroporosity, i.e., the parallel diffusional flux through micropores can be neglected [16]. Furthermore, at any position r, the concentration of benzene in the micropores may be assumed to be the same as that in the macroporosity, i.e., the diffusion out the microporosity is considered a fast phenomenon due to the small diameters of the single grains which all together compose the material. In fact, the diffusion time in the micrograins is estimated to be much smaller than the diffusion time in the sphere.

With the above assumption the diffusion of benzene in the sphere is governed by

$$\frac{\varepsilon D_s}{q}\left(\frac{\partial^2 c}{\partial r^2} + \frac{2}{r}\frac{\partial c}{\partial r}\right) = [\varepsilon + (1-\varepsilon)\varepsilon_i]\frac{\partial c}{\partial t} + \rho_b \frac{\partial \bar{c}}{\partial t}, \tag{3}$$

where the last term is the rate of absorption of benzene on the solid surface. If this rate is high with respect to diffusion, equilibrium is rapidly established at each point, i.e.,

$$\bar{c} = g(c), \tag{4}$$

Eq. (4) being the adsorption isotherm. For the purpose of this paper it may be assumed that:

$$\bar{c} = kc. \tag{5}$$

The initial and the boundary conditions to be associated with Eq. (3) are:

$$\text{(IC):} \quad \text{for} \quad t \leqslant 0, \quad c = c_0 \ \forall r, \tag{6}$$

$$\text{(BC1):} \quad \text{for} \quad r = 0, \quad \frac{\partial c}{\partial r} = 0 \ \forall t \geqslant 0, \tag{7}$$

$$\text{(BC2): for } r = R, \quad -\frac{D_s}{q}\frac{\partial c}{\partial r} = K_m(c(R) - c_\infty) \ \forall t \geqslant 0. \tag{8}$$

The concentrations in the right-hand side of Eq. (8) are liquid phase concentrations. $c(R)$ is the benzene concentration on the external surface of the sphere, and c_∞ is the benzene liquid phase concentration which would be required to maintain equilibrium with the benzene concentration C in the bulk gas. In general, for any volatile compound, the equilibrium relationship between gas phase and liquid phase concentration may be obtained by Raoult's law as

$$C = c\frac{p^v}{\Re T c_t} \tag{9}$$

where, for an ideal mixture it is

$$c_t = 1\Big/\sum_{i=1}^{n}\frac{x_i M_i}{\rho_i} + \frac{x_s M_s}{\rho_s}, \tag{10}$$

M_i and M_s are the molecular weight of the volatile compounds and of the solvent, respectively, and ρ_i and ρ_s are their densities.

K_m is the mass transfer coefficient in the gas film based on liquid phase concentration. Namely if K_g is the gas phase mass transfer coefficient, with reference to gas phase concentration (as calculated by the usual correlations) K_m is related to K_g by the following equation:

$$K_m = K_g\frac{p^v}{\Re T c_t}. \tag{11}$$

For brevity we set

$$E = [\varepsilon + \varepsilon_i(1 - \varepsilon) + \rho_b k] \tag{12}$$

and define the effective diffusivity as

$$D_e = \frac{(\varepsilon D_s/q)}{E}. \tag{13}$$

Substituting Eqs. (5) and (12) into Eq. (3), and using the definition of D_e we obtain

$$D_e\left(\frac{\partial^2 c}{\partial r^2} + \frac{2}{r}\frac{\partial c}{\partial r}\right) = \frac{\partial c}{\partial t}. \tag{14}$$

The solution of Eq. (14) with IC (6) and BCs (7) and (8) is given by Crank [17] as

$$\frac{c - c_\infty}{c_0 - c_\infty} = \frac{2\,Bi\,R}{r}\sum_{n=1}^{\infty}\frac{\exp(-D_e\beta_n^2 t/R^2)}{\{\beta_n^2 + Bi(Bi - 1)\}}\frac{\sin(\beta_n r/R)}{\sin\beta_n}. \tag{15}$$

The β_n's are the roots of

$$\beta_n\cot\beta_n + Bi - 1 = 0. \tag{16}$$

Bi is the Biot number and is introduced in Eq. (15) through BC (8). It is

$$Bi = \frac{K_m R}{D_s/q} \tag{17}$$

The instantaneous flux of the volatile leaving the sphere may be calculated from the expression

$$N = -\frac{\varepsilon D_s}{q}\frac{\partial c}{\partial r}\bigg|_{r=R}, \tag{18}$$

namely

$$N = 2\varepsilon\, Bi\, K_m[c_0 - c_\infty] \sum_{n=1}^{\infty} \frac{\exp(-D_e\beta_n^2 t/R^2)}{\beta_n^2 + Bi(Bi-1)}. \tag{19}$$

Eq. (19) accounts for both the diffusion in the particle and the mass transport through the gas film surrounding the particles. The Biot number is the indicator of which of the two resistances, internal, i.e., within the macroporal structure of the sphere, or external, i.e., across the gas film surrounding the sphere, controls the diffusion of volatile from liquid to gas. In particular, from the experimental data it is possible to infer that for $Bi \leqslant 1$ it is a good approximation to assume that external resistance controls the diffusion process. In this instance the concentration profile in the particle is flat ($c(R) \approx c(r=0)$). Therefore the rate of change of the concentration of the volatile in the sphere is described by the equation:

$$\frac{dc}{dt} = -\frac{3}{R}K_m(c - c_\infty) \tag{20}$$

with the IC $t = 0$, $c = c_0$. The solution of Eq. (20) is

$$\frac{c - c_\infty}{c_0 - c_\infty} = e^{-3K_m t/R}. \tag{21}$$

The flux leaving the sphere is

$$N = K_m\varepsilon(c - c_\infty) = K_m\varepsilon(c_0 - c_\infty)e^{-3K_m t/R}. \tag{22}$$

On the other side, when $Bi \gg 1$ (say $Bi \gg 10$) internal resistance prevails; i.e., $c(R) \approx c_\infty$. In this instance the concentration profile in the sphere is [17]

$$\frac{c - c_\infty}{c_0 - c_\infty} = -\frac{2R}{\pi r}\sum_{n=1}^{\infty}\frac{(-1)^n}{n}\sin\frac{n\pi r}{R}\exp(-D_e n^2\pi^2 t/R^2) \tag{23}$$

and the flux leaving the sphere is

$$N = \frac{2\varepsilon D_s}{qR}(c_0 - c_\infty)\sum_{n=1}^{\infty} e^{-D_e n^2\pi^2 t/R^2}. \tag{24}$$

Actually Eqs. (15) and (19) themselves contain Eqs. (21) and (22), and Eqs. (23) and (24). However, for computational purposes it is more convenient to use Eqs. (21) and (22) or Eqs. (23) and (24) when the conditions for their applicability prevail.

For the purposes of interpreting experimental data it is more worthwhile referring to the ratio of the total amount, $M(t)$, of the volatile leaving the sphere up to time t and the corresponding quantity, M_∞, after infinite time. This ratio is independent of concentration. The two quantities which enter the ratio are defined as

$$M(t) = 4\pi E \int_0^R [c_0 - c(r,t)] r^2 \, dr, \tag{25}$$

$$M_\infty = 4\pi E \int_0^R (c_0 - c_\infty) r^2 \, dr. \tag{26}$$

By applying these definitions to the three cases examined, we obtain

$$\frac{M(t)}{M_\infty} = 1 - \sum_{n=1}^{\infty} \frac{6Bi^2 \exp(-D_e \beta_n^2 t/R^2)}{\beta_n^2 [\beta_n^2 + Bi(Bi-1)]} \quad \text{for } Bi \approx 1, \tag{27}$$

$$\frac{M(t)}{M_\infty} = 1 - e^{-3K_m t/R} \quad \text{for } Bi < 1, \tag{28}$$

$$\frac{M(t)}{M_\infty} = 1 - \frac{6}{\pi^2} \sum_{n=1}^{\infty} \frac{1}{n^2} e^{D_e n^2 \pi^2 t/R^2} \quad \text{for } Bi \gg 1. \tag{29}$$

Again Eq. (27) contains in itself Eqs. (28) and (29). All of the above equations hold true for any volatile compound.

Bed of spheres

We must obtain a theoretical expression for $M(t)/M_\infty$ which will be used to fit the packed bed experimental data. For the bed of spheres, c is a function of r, t and z (the coordinate along the bed axis) while c_∞ is function of t and z. Therefore, a mass balance across a section of the bed of height dz must be considered to obtain an expression for $M(t)$. Setting n equal to the number of spheres per unit volume of the bed

$$M(t) = 4\pi E S n \int_0^L \int_0^R [c_0 - c(t, z, r)] r^2 \, dz \, dr. \tag{30}$$

Substituting for $c_0 - c(t, z, r)$ the value which may be obtained from Eq. (15) at any z, and integrating with respect to r we obtain

$$M(t) = 4\pi E S n \left[\frac{R^3}{3} \int_0^L (c_0 - c_\infty) \, dz - 2R^3 \sum_{n=1}^{\infty} \frac{Bi^2 \exp(-D_e \beta_n^2 t/R^2)}{\beta_n^2 [\beta_n^2 + Bi(Bi-1)]} \times \int_0^L (c_0 - c_\infty) \, dz \right]. \tag{31}$$

Correspondingly it is

$$M_\infty(t) = \frac{4\pi ESnR^3}{3} \int_0^L (c_0 - c_\infty)\,dz. \tag{32}$$

On dividing Eq. (31) by Eq. (32) we obtain for $M(t)/M_\infty(t)$ the same equation which holds true for the single sphere, i.e., Eq. (27). This result is not really surprising because we are considering a ratio and for spheres of the same dimension exposed to the same operating conditions, we can expect the ratio to be the same at any point in the bed for each t. The factors that affect the ratio $M(t)/M_\infty(t)$ are time, t, the effective diffusivity, D_e, and the Biot number Bi. At each t, the ratio is independent of the height, z, along the bed.

By using the same procedure, we conclude that the ratio $M(t)/M_\infty(t)$ for the packed bed is the same as that for single sphere, even for the cases of $Bi \ll 1$ and $Bi \gg 1$; i.e., Eqs. (28) and (29), respectively.

4. Interpretation of experimental results

4.1. Single sphere

The direct results obtained from the experimental apparatus are data points of benzene concentration in the outlet nitrogen stream with time. They are reported in the thesis by Savino [12]. For the purposes of interpreting experimental data it is more worthwhile referring to the term $M(t)/M_\infty$ which is independent of concentration. Therefore the concentration with time data is worked out in terms of $M(t)/M_\infty$ which is given by the relationship:

$$M(t) = Q \int_0^t C_{ex}\,dt, \tag{33}$$

where Q is the nitrogen flow rate and C_{ex} is the benzene concentration in the syringe samples. Thus $M(t)$ is calculated by numerical integration of the experimental C_{ex} vs. t data points. In fact, during the experiments the gas flowrate is frequently monitored so as to maintain it constant.

M_∞ is defined by Eq. (26) where for the experiments with the single sphere it is $c_\infty = 0$ as the experiments are performed in a differential desorber. There are two independent ways to determine the experimental value of M_∞. The first is by the weighing procedure (M_∞ is just the weight of benzene initially loaded in the sphere). The second, based on Eq. (33) is by integrating the concentration vs. time plot from $t = 0$ to $t = t_f$ obtaining $M(t_f)$. It resulted for all runs $M_\infty \approx M(t_f)$ in a range of $\pm 10\%$. In the calculations we have used the first value of M_∞. As an example, the results for runs Sp-1, Sp-2 and Sp-4 are reported in Fig. 2.

In order to compare the experimental results with the model equations, it is necessary to know the numeric values of a few parameters. As regards the porosity and the density, which are characteristic of the specific system under study, they have

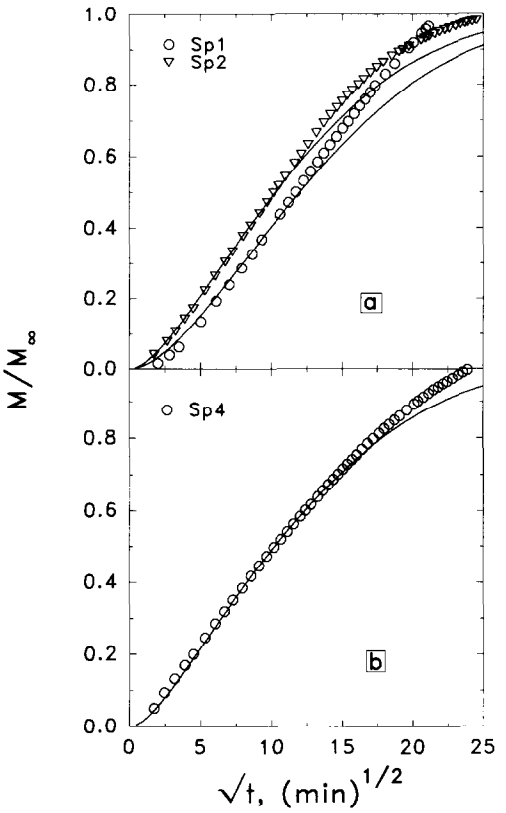

Fig. 2. Release of benzene from a sphere ($R = 1.35$ cm) of porous material imbued with a mixture of benzene in tetradecane. (a) The porous material is sinterized SS, the benzene mole fraction x_b and the nitrogen flow rate Q are: $x_b = 0.1$ and $Q = 1$ ml/s for run Sp-1; $x_b = 0.2$ and $Q = 10$ ml/s for run Sp-2. (b) The porous material is a tuff rock; $x_b = 0.2$; $Q = 10$ ml/s. In both figures the curves through the data are Eq. (27).

been evaluated experimentally according to standard procedures and/or instruments and are reported in Table 1.

Other parameters can be readily and confidently estimated from results reported in the literature. They are the following:

Free diffusivity of the diffusing chemical. There exist reliable correlations [18, 19] that enable us to evaluate with reasonable accuracy the free diffusivity.

Gas-phase mass transfer coefficient. The mass transfer coefficient in the gas film may be predicted from the correlation [20]:

$$Nu = 2 + 0.6(Re)^{1/2}(Sc)_f^{1/3}, \tag{34}$$

where

$$Nu = \frac{K_g(2R)}{D_N}, \quad Re = \frac{(2R)v_\infty \rho_f}{\mu_f}, \quad (Sc)_f = \frac{\mu_f}{\rho_f (D_N)_f}. \tag{35}$$

The most questionable parameter to be determined is the tortuosity. Specific instruments to measure it are not available. Inspection of the many experimental values which have accumulated in the literature [21] shows that the majority of the tortuosity values for porous catalysts ranges between 1 and 3. Therefore, the only possibility to obtain a closer estimate of q is to perform diffusion experiments directly on the porous solid of interest and evaluating the tortuosity as an adjustable parameter to fit the experimental data. This is the procedure that we have followed. As a matter of fact we have preferred to evaluate directly the effective diffusivity by the best fit procedure.

Eq. (27) is utilized to fit the data. Two parameters must be determined by the fitting procedure, i.e., D_e which appears in the exponential term and the Biot number. First the SS porous sphere data are analyzed. For this porous material it may be safely assumed that both microporosity and adsorption phenomena are absent. Therefore it is $D_e = D_s/q$. Thus by determining the fitting values of D_e and Bi one eventually determines D_s/q and K_m (through the Biot number, Eq. (17)). The determination of K_m is useful to check the accuracy of the predicting equation for the mass transfer coefficient (Eq. (34) with Eqs. (35) and (11)). In all cases the results indicate that the predicting equations give a good estimate of K_m.

Then the data regarding the two types of rock tuff are analyzed and the fitting values of D_e and Bi are determined for each run. In this case, however, K_m is calculated by the predicting equation. Therefore, the fitting procedure allows us to determine separately D_e and D_s/q. It results that for all runs $D_e \approx D_s/q$. Thus $\varepsilon_i(1-\varepsilon) + \rho_b k \ll \varepsilon$ and $E \cong \varepsilon$. Thus, even for the tuff rock, microporosity and adsorption do not have a significant effect on diffusion.

Table 2 summarizes the results of the fitting procedure. In Fig. 2 the solid curves through the data are Eq. (27). The discrepancy between data and curves at high values of t are due to numerical errors during the integration of C_{ex} by Eq. (33) when the outlet concentration becomes exceedingly low. The plots for the other Sp runs are given in a thesis by Savino [12].

4.2. Packed bed

The direct results obtained from the experimental apparatus are data points of volatile concentrations in the outlet gas stream with time. They are reported in the thesis by Saha [13]. As for the single sphere experiments, the term $M(t)/M_\infty$ is used to describe the mass transfer process occurring across the bed.

The values of the parameters D_e and K_m that are used to fit the experimental results are as follows: The effective diffusivity used for the benzene data is that determined from the single sphere experiments using yellow tuff, i.e., $D_e = D_s/q = 1.4 \times 10^{-5}$ cm^2/s. The same value of D_e, as that for benzene is used for chlorobenzene and

Table 2
Biot numbers for the various runs

Run no.	D_e (cm^2/s)	ϕ	$(Bi)_b$	$(Bi)_{cl}$	$(Bi)_{dcl}$
Sp-1	1.45×10^{-5}	1.0	6.4	—	–
Sp-2	1.55×10^{-5}	1.0	12	—	—
Sp-3	1.12×10^{-5}	1.0	20	—	—
Sp-4	1.40×10^{-5}	1.0	16	—	—
Pb-1	(1.40×10^{-5})	2.5	18.8	—	—
Pb-2	(1.40×10^{-5})	2.5	19.7	2.1	—
Pb-3	(1.40×10^{-5})	1.0	—	0.9	—
Pb-4	(1.40×10^{-5})	2.5	—	2.3	—
Pb-5	(1.40×10^{-5})	2.5	—	2.1	0.4
Pb-6	(1.40×10^{-5})	2.5	18.8	2.0	0.3
Pb-7	(1.40×10^{-5})	2.5	23.3	2.6	0.5

The K_m entering the Biot numbers are calculated by Eqs. (34) and (11) for Sp runs. By Eqs. (36) and (11) for Pb runs; D_e 's in parentheses indicate assumed values.

dichlorobenzene. This is because the free diffusivity of chlorobenzene and dichlorobenzene in tetradecane, calculated using the predicting equations proposed by Reid et al. [18], is found to differ very little from that of benzene. The tortuosity coefficient remains the same because this depends on the porous material used. Knowing the other physical parameters that are applicable to our system, we calculate K_g, the mass transfer coefficient in the gas phase with reference to gas phase concentrations, expressed in units of cm/s, using the j_D-factor [20]:

$$j_D = \frac{K_g \rho}{G}(Sc)^{2/3}. \tag{36}$$

For a packed bed operated at low Reynolds numbers, as those prevailing in our experiments, the following equation is suggested by Bar–Ilan and Resnick [22]:

$$j_D = 0.6(Re)^{-0.46} \quad \text{for } 1 < Re < 250, \tag{37}$$

where the Reynolds number is defined as

$$Re = \frac{(2R)G}{\mu}, \tag{38}$$

K_m is then calculated by Eq. (11). The Biot numbers obtained by the calculation procedure are reported in Table 2.

Before progressing any further with the interpretation of data, we must consider a finding which is specific to the packed bed experiments. These experiments showed that pockets of liquid may come to be trapped in the bed voidage. This peculiarity is also found by Thibodeaux and Hwang [1]. This phenomenon has the effect of elongating the diffusion length. As far as the diffusion process is concerned the bed

behaves as if it were filled with particles having a diameter larger than that of the actual spheres. This effect can be accounted for by introducing a clustering factor ϕ ($\phi > 1$) and defining the equivalent radius as $R_e = \phi R$. For our packed bed this factor is evaluated to be $\phi = 2.5$. Runs Pb-3 and Pb-4 were performed for the specific purpose of checking the validity of our explanation for the need of a clustering factor. In run Pb-3, before insertion into the desorption chamber, the wet spheres in the bed were scattered in order to free any trapped liquid. Run Pb-4 however followed the normal experimental procedure (see Table 1). The results obtained verify the theory put forward to account for the clustering factor, i.e., when the bed voidage is free of the liquid mixture the clustering factor is not relevant as the characteristic diffusion length of the spheres, R, is not elongated. This verification experiment was carried out using chlorobenzene instead of benzene because the high volatility of benzene would have meant the immediate loss to the atmosphere of a significant fraction of benzene when the spheres were scattered. Therefore, the diffusion equations discussed in Section 3, when applied to the packed bed arrangement, must have an R_e in place of R wherever it appears.

For the packed bed experiment the procedure for obtaining the $M(t)/M_\infty$ ratio from the raw data is more involved than for the case of the single sphere. The value of $M(t)$ calculated from experimental results is obtained according to Eq. (33).

M_∞ should be calculated by Eq. (32) where, the term $4\pi EnR^3/3$ is the total free volume per unit volume of the bed available within the spheres to absorb liquid. The total free volume of all spheres in the bed is obtained knowing the mass of liquid absorbed by the spheres, M_a, prior to the experimental run and the density of the liquid mixture absorbed, ρ_t

$$\frac{4\pi R^3 ESLn}{3} = \frac{M_a}{\rho_t}, \tag{39}$$

SLn is the total number of spheres loaded in the desorber.

A problem, however arises when Eq. (32) must be utilized. In fact, the c_∞ term is a function of t and z because the bed of spheres behaves as an integral desorber. In order to calculate M_∞, a suitable method to evaluate c_∞ has to be decided upon, based on the measured results obtained during the experiment, i.e., the variation of C_{ex} with time. The experimental results used to set the method for evaluating M/M_∞ are those for run Pb-1 which is reported in Fig. 3.

Considering the volatile concentration in the bulk gas within the bed, C, we can say that at $z = 0$, $C = 0$ because the incoming gas flow has not yet come into contact with the wet spheres. At $z = L$ however $C = C_{ex}$ because that is the concentration measured in the exit gas. Therefore we can rightly make the conclusion that C in the bed must vary between these two extremes or outer limits.

We are now in a position to consider the two limiting cases for the variation of C along the height of the bed: (1) $C = 0$, i.e., C remains 0 through most of the bed and only reaches the value of C_{ex} at $z = L$. (ii) $C = C_{ex}$, i.e., the exit concentration is instantaneously reached at $z = 0$ and remains at this value throughout the height of the bed.

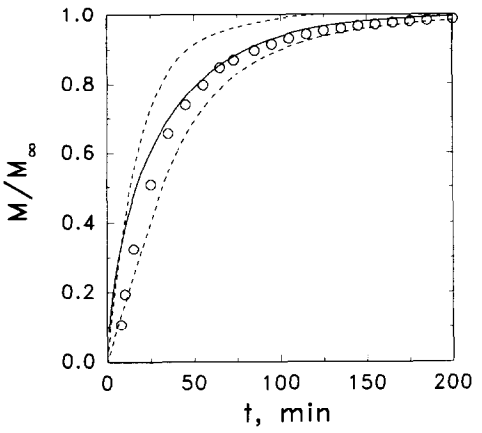

Fig. 3. Run Pb-1. Release of benzene from a bed of rock tuff spheres (R = 0.22 cm) imbued with a mixture of benzene in tetradecane (x_b = 0.2). The height of the bed is L = 6.2 cm. The dashed curves are the locations of the experimental data if they were worked out using the two limiting gas phase concentrations: $C = C_{ex}$ (upper curve); $C = 0$ (lower curve). The circle symbols are the experimental data worked out with $C = C_{ex}/2$. The solid curve is Eq. (27).

The actual behaviour of C in our system would have to lie somewhere in between these two limits. The two limiting M_∞ values were calculated using Eq. (32) and (9) which relates C to c_∞. Thus the experimental M/M_∞ vs. t data, based on the two limiting M_∞ values, were calculated. They are reported as dashed curves in Fig. 3. The two curves obtained are quite close to each other.

The theoretical M/M_∞ curve (solid curve in Fig. 3), obtained using Eq. (27), is plotted for the same operating conditions and is found to fit in between the two outer limit curves, see Fig. 3. The only modification to the theoretical equation for M/M_∞ is the introduction of the clustering factor $\phi = 2.5$ in the Biot number and in the exponent of Eq. (27).

Based on the result that the experimental outer limit curves are quite close to each other, we tried the hypothesis that $C = C_{ex}/2$. This hypothesis assumes that the concentration profiles along the bed can be approximated by considering linearity with respect to z.

On making the aforementioned hypothesis, the value of c_∞ at each t could then be calculated using Eq. (9) in which C is replaced by $C_{ex}/2$ whose variation with t is directly obtained from experiment. This method was used to evaluate the M_∞ term (Eq. (32)) obtaining the M/M_∞ data shown as circle symbols in Fig. 3. The good agreement between the experimental and theoretical curve suggests that the actual concentration profile is not too different from the linear approximation used. Therefore the method was used to evaluate the M_∞ term for all the experimental runs.

Inspection of Eqs. (11) and (17) and the results of Table 2 show that the Biot number varies according to the volatility of the compound. As compound volatility decreases a greater role is played by the external resistance than internal resistance in

controlling the diffusion process. For example, the experiments show that when all three components are simultaneously present in the tetradecane it happens that the diffusion of benzene (p^v = 75 mmHg at 19 °C) is internally controlled, that of chlorobenzene (p^v = 8.4 mmHg at 19 °C) is both internally and externally controlled, while that of dichlorobenzene (p^v = 1.5 mmHg at 19 °C) is externally controlled.

Therefore, we will first discuss the results regarding benzene and chlorobenzene and finally the dichlorobenzene results. This time, because all parameters of the Eq. (27) are predetermined, the fitting is not by trial.

Benzene results. Runs Pb-(1, 2, 6, 7). The M/M_∞ data are interpreted by Eq. (27). In this equation in place of R wherever it appears, the equivalent radius R_e is considered ($R_e = \phi \cdot R$, $\phi = 2.5$). The data and the fitting curve for run Pb-7 are reported as an example in Fig. 4. The agreement between the benzene data and the solid curves (which represent Eq. (27)) indicate the accuracy of the predicting equation used to fit the data. The same agreement is found for the benzene data of all other runs in which this component is present.

Chlorobenzene results. The diffusion of chlorobenzene is analysed in runs Pb-(2, 3, 4, 5, 6, 7). It is the only volatile component present in runs Pb-3 and Pb-4. In run Pb-2 it is present together with benzene. In run Pb-5 chlorobenzene and 1,3-dichlorobenzene are the two volatiles presents. In runs Pb-6 and Pb-7, all three volatiles are present together, but run Pb-7 has a smaller bed height, L = 2 cm.

Inspection of the *Bi* values of Table 2 indicate that the release of chlorobenzene has mixed control. The chlorobenzene data are then interpreted by using Eq. (27). In all cases we find good agreement between the data points (M/M_∞ vs. $\sqrt{t}$) and the solid

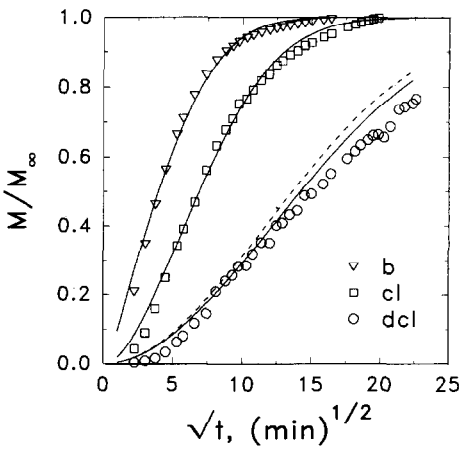

Fig. 4. Run Pb-7. Simultaneous release of benzene (b), chlorobenzene (cl) and dichlorobenzene (dcl) from a bed of rock tuff spheres (R = 0.22 cm) imbued with a mixture of the three volatiles in tetradecane. The solid curves are Eq. (27); the dashed curve through the dichlorobenzene data is Eq. (28). The height of the bed is L = 2 cm.

curves (Eq. (27)). As an example the results of the fitting procedure for the chlorobenzene data of run Pb-7 are reported in Fig. 4.

Dichlorobenzene results. The diffusion of 1,3-dichlorobenzene is analysed in runs Pb-(5, 6, 7). In run Pb-5, it is present in the liquid mixture with chlorobenzene. In runs Pb-6 and Pb-7, however all three volatiles are present in the liquid mixture. The experimental runs carried out in Runs Pb-5 and Pb-6 have a bed height, $L = 6.2$ cm.

The experimental M/M_∞ ratio is evaluated following the same methodology as used for benzene and chlorobenzene. Inspection of the *Bi* values reported in Table 2 let us assume that the external resistance controls the diffusion of 1,3-dichlorobenzene into gas. Thus the dichlorobenzene data are analyzed by Eq. (29). When the fitting is attempted for the dichlorobenzene data of runs Pb-5 and Pb-6 we find that the two experimental M/M_∞ ratios climb at a much slower rate than their theoretical counterparts. Therefore the expected diffusion process is being retarded by some other phenomenon. A simple mass balance across the bed shows that the gas flowing through the bed reaches (as far as dichlorobenzene is considered) equilibrium concentration well before $z = L$. As a matter of fact, equilibrium concentration is already reached in the bed at a height of 4 cm and is a limiting factor in the diffusion of 1,3-dichlorobenzene into the gas. This explains the slow rate at which the experimental M/M_∞ curves climb with respect to the theoretical curves for both run 5 and run 6.

For the other volatile components in run Pb-5 (chlorobenzene) and in run Pb-6 (chlorobenzene and benzene) this phenomenon does not take place because internal resistance plays a much more influential part in the diffusion process of these two components. In fact, the chlorobenzene and benzene data for the runs Pb-5 and Pb-6 are well described by Eq. (27). The internal resistance, $\phi R/D_e$ controls the flux in such a way that equilibrium concentrations are not reached.

Based on the above finding that for 1,3-dichlorobenzene, equilibrium concentrations are reached in the bed for height $L = 6.2$ cm, we decided to carry out another experimental run, run Pb-7, using a much smaller bed height. The calculation had shown that the bed height needed to be less than 4 cm to avoid saturation. Therefore $L = 2$ cm was chosen. This run was performed using all three volatile components. The M/M_∞ theoretical (Eq. (27)) and experimental plots are shown in Fig. 4. With regard to the dichlorobenzene fitting, the dashed curve represents Eq. (29) while the solid one is Eq. (27). The closeness of both curves lends further support to our conclusion about external resistance control of the diffusion of 1,3-dichlorobenzene.

5. Discussion and conclusions

The theoretical and experimental analysis presented in this paper shows that the available theoretical tools for the study of diffusion can be safely used to obtain accurate modeling of the air emission release rate of hazardous chemicals from porous materials. The experiments have been conducted with closely controlled geometry, porous structure and nature of the porous material, and fluid dynamics, so as to reduce to a minimum the uncertainties in the predictive equations and focus attention

on the role played by the transport phenomena taking place inside the porous particles. In particular, the release of different volatiles, having a large spectrum of volatilities, from porous spheres has been studied. The use of the models entails the determination of basic parameters which frequently occur in well-investigated areas of chemical engineering. In particular it has been highlighted that special diffusive phenomena like surface migration do not play a sensible role in the process, in agreement also with the conclusions of Dupont [2]. The parameters required to predict the air release of toxic chemicals from porous materials may be roughly divided into two categories.

The first category regards parameters which are characteristic of the specific system under study and have to be evaluated experimentally according to standard procedures and/or instruments (i.e., tortuosity, porosity).

The second category considers parameters which can be readily and confidently estimated from the data reported in literature. They are: (i) free diffusivity of the diffusing chemical; (ii) gas phase mass transfer coefficients.

Moreover, the packed bed experiments have shown that pockets of liquid may come to be trapped in the bed voidage. As far as the diffusion process is concerned the bed behaves as it were filled with particles having a diameter larger than that of the actual spheres. This effect can be accounted for by introducing a clustering factor ϕ ($\phi > 1$) and defining the equivalent radius as $R_e = \phi R$. For our packed bed it has been evaluated at $\phi = 2.5$. For the single sphere it is $R_e = R$. It is not possible with the data at hand to infer on the dependency of ϕ on the particle diameter.

Finally, it has been shown that as the volatility decreases the greater the role played by the external resistance in controlling the diffusion process. For example, the experiments show that when all three components are simultaneously present in the tetradecane it happens that the diffusion of benzene ($p^v = 75$ mmHg at 19 °C) is internally controlled, that of chlorobenzene ($p^v = 8.4$ mmHg at 19 °C) is in a mixed control regime, while that of dichlorobenzene ($p^v = 1.5$ mmHg at 19 °C) is externally controlled.

Nomenclature

Bi	Biot number, see Eq. (17)
$\bar{c}$	adsorbed concentration of the volatile on the solid surface, mol/g
c	liquid phase concentration of the volatile in the porous solid, mol/ml
c_t	total liquid phase concentration, see Eq. (10), mol/ml
c_∞	liquid phase concentration required to maintain equilibrium with the surrounding bulk gas (from Eq. (9)), mol/ml
C	gas phase concentration of the volatile, mol/ml
D_e	effective diffusivity in porous solid; see Eq. (13), cm^2/s
D_N	gas phase diffusivity of volatile in nitrogen, cm^2/s
D_s	free diffusivity of volatile in solvent (tetradecane), cm^2/s
E	see Eq. (12)

G mass velocity of gas based on total bed cross section, g/(cm^2 s)
j_D j factor for mass transfer, see Eq. (37)
k adsorption equilibrium constant, see Eq. (5), ml/g
K_g mass transfer coefficient based on gas phase concentration, cm/s
K_m mass transfer coefficient, based on liquid phase concentration, cm/s
L bed height, cm
M total amount of diffusing volatile leaving the sphere up to time t, mol
M_∞ total amount of diffusing volatile leaving the sphere after infinite time, mol
M_a mass of liquid absorbed by the spheres, g
M_i molecular weight of compound, g/mol
M_s molecular weight of solvent, g/mol
n number of spheres per unit volume of bed
N mass flux referred to the total area, mol/(cm^2 s)
Nu mass transfer Nusselt number, see Eq. (35)
p^v vapor pressure of diffusing compound, atm
q tortuosity
Q volumetric flow rate at room temperature and 1 atm, ml/s
r radial coordinate, cm
r_c pore radius, Å
R radius of the sphere, cm
$\Re$ gas constant (= 82.057 atm ml/(mol K)
R_e equivalent radius (= ϕR), cm
Re Reynolds number, see Eq. (35) or (38)
S bed cross-sectional area, cm^2
Sc Schimdt number in air for volatile component, see Eq. (35)
t time, s
t_d characteristic time for diffusion, s
t_f final time of the run, s
T temperature, K
v_∞ average velocity around the sphere, cm/s
x_b liquid phase molar fraction of benzene
x_i liquid phase molar fraction of volatile
x_s liquid phase molar fraction of solvent
z coordinate along the bed axis, cm

Greek symbols

β_n see Eq. (16)
ε intraparticle macroporosity
ε_i intraparticle microporosity
ε_t total intraparticle porosity
μ nitrogen viscosity, g/(cm s)
ρ nitrogen density at room temperature and 1 atm, g/ml
ρ_b bulk density of the porous solid, g/ml
ρ_i density of compound i, g/ml

ρ_p true density of the powder of which the porous solid is made, g/ml
ρ_s density of solvent (tetradecane), g/ml
ρ_t density of liquid mixture, g/ml
ϕ clustering factor

Subscripts

b benzene
f properties evaluated at the "film composition"
ex out of the desorber
i any volatile
0 initial
s solvent (tetradecane)

Acknowledgements

This work was financed by research grants from "Ministero dell'Università e della Ricerca Scientifica e Tecnologica" and from "Consiglio Nazionale delle Ricerche". "La Nuova Merisinter" is to be acknowledged for providing the sinterized stainless steel. We wish to thank Prof. G. Mascolo for providing us with the tuff rock and the pore size distribution curve for the yellow tuff.

References

[1] L.J. Thibodeaux and S.T. Hwang, Landfarming of petroleum wastes-modeling the air emission problem, Environ. Prog., 1 (1982) 42–46.
[2] R.R. Dupont, Evaluation of air emission release rate model predictions of hazardous organics from land treatment facilities, Environ. Progr., 5 (1986) 197–206.
[3] A.A. Karimi, W.J. Farmer and M.M. Cliath, Vapor-phase diffusion of benzene in soil, J. Environ. Qual., 16 (1987) 38–43.
[4] W.J. Grenney, C.L. Caupp, R.C. Sims and T.E. Short, A mathematical model for the fate of hazardous substances in soil: model description and experimental results, Hazard. Waste and Hazard. Mater., 4 (1987) 223–239.
[5] L.J. Thibodeaux, K.T. Valsaraj, C. Springer and G. Hildebrand, Mathematical models for predicting chemical vapor emission from landfills, J. Hazard. Mater., 19 (1988) 119–123.
[6] G. Eduljee, Volatility of TCDD and PCB from soil, Chemosphere, 16 (1987) 907–920.
[7] A. Karimi, V. Ravindran and M. Pirbazari, A laboratory experiment and predictive model for evaluating landfill cover controls of emissions of volatile organic chemicals to air, Hazard. Waste Hazard. Mater., 5 (1988) 203–218.
[8] R.G. Nash and T.H. Gish, Halogenated pesticide volatilization and dissipation from soil under controlled conditions, Chemosphere, 18 (1989) 2353–2362.
[9] R.G. Nash, Models for estimating pesticide dissipation from soil and vapor decline in air, Chemosphere, 18 (1989) 2375–2381.
[10] W.D. Balfour, R.G. Wetherold and D.L. Lewis, Evaluation of air emissions from hazardous waste treatment, storage, and disposal facilities, EPA Project Summary, EPA/600/S2-85/057, July 1985.

[11] W. Blumberg, and E.-U. Schlünder, Simultaneous vapor and liquid diffusion in partially wetted porous media, Drying Technol., 11 (1993) 41–64.
[12] G. Savino, Meccanismi di rilascio nell'atmosfera di composti tossici contenuti in materiali porosi, Tesi di Laurea in ingegneria chimica, Napoli, Italy, 1992.
[13] P. Saha, The release of toxic volatiles into the atmosphere from porous media held in a packed bed arrangement, M. Chem. Eng. Thesis, Napoli, Italy, 1993.
[14] R.J. MIllington and J.M. Quirk, Permeability of porous solids, Trans. Faraday Soc., 57 (1961) 1200–1207.
[15] A.S. Foust, L.A. Wenzel, C.W. Clump, L. Maus and L.B. Andersen, Principles of Unit Operations, Wiley, New York, 1960.
[16] N. Vakao and J.M. Smith, Diffusion in catalyst pellets, Chem. Eng. Sci., 17 (1962) 825–834.
[17] J. Crank, The Mathematics of Diffusion, 2nd edn., Clarendon Press, Oxford, UK, 1975, pp. 91, 96.
[18] R.C. Reid, J.M. Prausnitz and T.K. Sherwood, The Properties of Gases and Liquids, 3rd edn., McGraw-Hill, New York, NY, 1977.
[19] Perry's Chemical Engineers' Handbook, 5th edn., McGraw-Hill, New York, NY, 1984.
[20] R.B. Bird, W.E. Stewart and E.N. Lightfoot, Transport Phenomena, Wiley, New York, 1965, p. 647.
[21] C.N. Satterfield and T.K. Sherwood, The Role of Diffusion in Catalysis, Addison-Wesly, Reading, MA, 1963.
[22] M. Bar-Ilan, W. Resnick, Gas phase mass transfer in fixed beds at low Reynolds numbers, Ind. Eng. Chem., 49 (1957) 313–320.